Materials Chemistry and Physics 136 (2012) 638–647

Contents lists available at SciVerse ScienceDirect

Materials Chemistry and Physics

journal homepage: www.elsevier.com/locate/matchemphys

Oxidation study on as-bonded intermetallic of copper wire–aluminum bond pad metallization for electronic microchip

T. Joseph Sahaya Anand [a,*], Chua Kok Yau [a,b], Lim Boon Huat [c]

[a] Faculty of Manufacturing Engineering, University Technical Malaysia Melaka, Hang Tuah Jaya, 76100 Durian Tunggal, Melaka, Malaysia
[b] University of Technical Malaysia Supported by Infineon Technology (Malaysia) Sdn. Bhd., Melaka, Malaysia
[c] Department of Innovation, Infineon Technology (Malaysia) Sdn. Bhd., FTZ Batu Berendam, 75350 Melaka, Malaysia

HIGHLIGHTS

- 3 nm Al_4Cu_9 are found in sample prepared with Forming Gas ON.
- 15 nm mixed CuAl + $CuAl_2$ are found in sample prepared with Forming Gas OFF.
- Voids are present at the bonding interfaces of both samples.
- Both samples have similar ball shear strength.
- Estimated interfacial temperature of as-bonded Forming Gas ON sample ~437 °C.

ARTICLE INFO

Article history:
Received 27 October 2011
Received in revised form
5 June 2012
Accepted 21 July 2012

Keywords:
Intermetallic compounds
Energy dispersive analysis of X-rays
Oxidation
Electron microscopy (TEM and SEM)

ABSTRACT

In this work, influence of Copper free air ball (FAB) oxidation towards Intermetallic Compound (IMC) at Copper wire–Aluminum bond pad metallization (Cu/Al) is studied. Samples are synthesized with different Copper FAB oxidation condition by turning Forming Gas supply ON and OFF. Studies are performed using Optical Microscope (OM), Scanning Electron Microscope (SEM), Transmission Electron Microscope (TEM) and line-scan Energy Dispersive X-ray (EDX). SEM result shows there is a cross-sectional position offset from center in sample synthesized with Forming Gas OFF. This is due to difficulty of determining the position of cross-section in manual grinding/polishing process and high occurrence rate of golf-clubbed shape of oxidized Copper ball bond. TEM inspection reveals that the Copper ball bond on sample synthesized with Forming Gas OFF is having intermediate oxidation. Besides, the presence of IMC at the bonding interface of Cu/Al for both samples is seen. TEM study shows voids form at the bonding interface of Forming Gas ON sample belongs to unbonded area; while that in Forming Gas OFF sample is due to volume shrinkage of IMC growth. Line-scan EDX shows the phases present in the interfaces of as-bonded samples are Al_4Cu_9 (~3 nm) for sample with Forming Gas ON and mixed CuAl and $CuAl_2$ (~15 nm) for sample with Forming Gas OFF. Thicker IMC in sample with Forming Gas OFF is due to cross-section is positioned at high stress area that is close to edge of ball bond. Mechanical ball shear test shows that shear strength of sample with Forming Gas OFF is about 19% lower than that of sample with Forming Gas ON. Interface temperature is estimated at 437 °C for as-bonded sample with Forming Gas ON by using empirical parabolic law of volume diffusion.

1. Introduction

Copper (Cu) wire bonding has been extensively developed to replace expensive Gold wire material since 80 s in semiconductor industry [1,2]. Cu material has better heat and electrical conductivity (398 $Wm^{-1}K^{-1}$ and 6.0 × 10^7 $\Omega^{-1}m^{-1}$ [3], respectively) that are suitable for high power and faster chip functionality [4]. Besides, Cu material possesses higher Young's Modulus (110 GPa [3]) which helps in reducing the sagging wire problem during manufacturing process [4].

In semiconductor industry, Aluminum (Al) bond pad metallization is commonly deposited on the microchip. It serves as the Input/output terminal (I/O) that connects external circuit through the bonded wires. Cu wire–Al bond pad metallization material combination (Cu/Al) has been extensive studied [5–7]. Some of the studies report the manufacturing challenge with this material

* Corresponding author.
E-mail address: anand@utem.edu.my (T. Joseph Sahaya Anand).

0254-0584/$ – see front matter © 2012 Elsevier B.V. All rights reserved.
http://dx.doi.org/10.1016/j.matchemphys.2012.07.036

combination, such as excessive Al deformation or Al "splash" and damage under the bond pad metallization, due to scrubbing and impact of harder Cu wire towards soft Al [8–10]. Al splash will bring risk of short circuit if the splashed Al touches an adjacent bond pad [9]. Damage under bond pad metallization is caused by Al splash that decreases the Al bond pad thickness at the high stress region and in turn causing cracking at the structures underneath the bond pad [10]. However, reduced process parameters to minimize the occurrence of the defects may significantly decrease the shear strength of the Cu/Al bonding. These challenges limit the process window of Cu wire bonding [9].

Thermosonic (Thermal + Ultrasonic) wire bonding technique is a well-known interconnection method in the industry to fuse the wire material onto bond pad metallization on a microchip [11,12]. This technique has been discussed in detail in a review paper of [10] which could be summarized as follows: "a Free Air Ball (FAB) is first formed in Electric Frame Off (EFO) process that uses electrical sparks to melt the wire tip into a symmetrical sphere. The FAB is then compressed by a capillary against the bond pad metallization with a preset force and ultrasonic power. Ultrasonic vibration causes softening of the FAB and thus its plastic deformation. Scrubbing between FAB and bond pad metallization removes contamination and oxides on metallization surface and form new intermetallic phase at the interface. This new phase anchors the FAB and bond pad metallization which promoting bonding at the interface".

Due to the nature of Cu that is easily oxidized, the EFO must be done in an inert environment (usually Forming Gas with 95% N_2 + 5%H_2) [5]. Oxidized Cu FAB tends to cause wire bonding process difficulty, e.g. cratering which the ball bond lifts from the surface of the bond pad metallization with a portion of material of bond pad and underlying oxide or silicon [6]. In this context, a feature that supplies Forming Gas flow around the EFO region is introduced and termed as "Copper Kit" [5]. Most of the modern wire bonders are compatible for installation of the Copper kit. This feature consists of simple tubing that guides the Forming Gas flow towards EFO region from different directions. It is normally an open design due to constraint of bond head movement. Though Copper kit is essential for industrial Cu wire bonding process, however, its open to environment design will easily allow severe or partial oxidation of Cu FAB to occur if the flow rate of Forming Gas is not optimized or stable for long service duration. One could notice that research on oxidized Cu in wire bonding is limited because of little interest of engineer/researcher to study such failure. This may limit the understanding of influence of oxidation towards Cu wire bonding.

In this paper, the influence of FAB oxidation toward the mechanical performance and also interfacial characteristic, including mechanical strength, voiding and formation and growth of the IMCs around the bonding interface of as-bonded Cu/Al sample is studied. Micro-structural and chemical characterization is carried out by using optical microscope (OM), scanning electron microscope (SEM), transmission electron microscope (TEM) and line-scan Energy Dispersive X-ray (EDX) (equipped in TEM). Mechanical strength is measured using industrial ball shear tester. This approach leads to better understanding on the effect of FAB oxidation towards the Cu wire bonding quality.

2. Experimental procedures

Diode microchips with pure Al bond pad metallization were first transferred from wafer to leadframe by normal die bonding process. Then the samples were bonded with 22 μm 5N (purity of 99.999%) Cu wire. The wire bonding process was carried out on a commercially available Shinkawa ACB-35 wire bonder with Cu kit from the machine maker. The bonding parameters including forming gas flow rate were fine-tuned to ensure no bonding issue e.g. Non Stick On Pad (NSOP) and Cu FAB oxidation. Table 1 summarizes the optimized and established wire bonding parameters used in the sample fabrication. After fine-tuning and quality verification, 2 groups of samples were synthesized at bonding temperature at 280 °C, i.e.

a) with Forming Gas flow ON, and
b) with Forming Gas flow OFF, to facilitate the worst oxidation condition of Cu FAB.

Table 1
Optimized wire bonding parameters used in the experiment.

Parameters	Setting
Ultrasonic power (unit)	30
Bond force (gf)	30
Bonding time (ms)	15
Bonding temperature (°C)	280

The samples with successful bonding were sent for shear test to measure the shear force of Cu/Al bonding. Equipment used in this case is DAGE series 4000 ball shear tester. Cu ball bond was etched away by using HCl acid, prior to bonding area determination using high power OM. Ball shear strength was then calculated by force/bonding area. For microstructure examination, some samples were sent for mechanical cross-section so that the interface of Cu wire, Cu ball bond and Al bond pad metallization are visible. Cross-section was performed in a direction perpendicular to that of ultrasonic vibration during Thermosonic Bonding process. Next, the cross-sectioned samples were proceeded with Nova Lab focus ion beam (FIB) for lamella preparation (dimension ~ 10 μm × 10 μm × 0.1 μm) that was taken from the center of the cross-section samples of each category. Micro-structure and chemical characterization will be carried out using EFI CM200 TITAN TEM and JEOL-LV/EDX SEM that equipped with EDX feature.

3. Results and discussion

SEM images of sample with Forming Gas ON and OFF are shown in Figs. 1 and 2, respectively. In Fig. 1, Al bond pad at both left and right ends of Cu ball bond experience smearing during grinding/

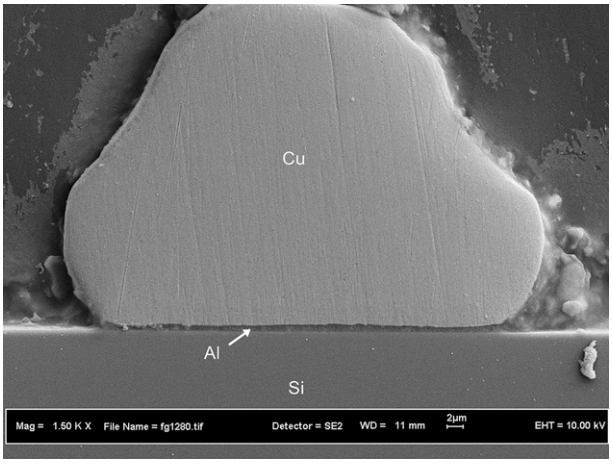

Fig. 1. Cross-sectional SEM image of Cu wire bonded sample fabricated with forming gas ON. Al smearing during grinding/polishing is observed at left and right ends of the ball bond.

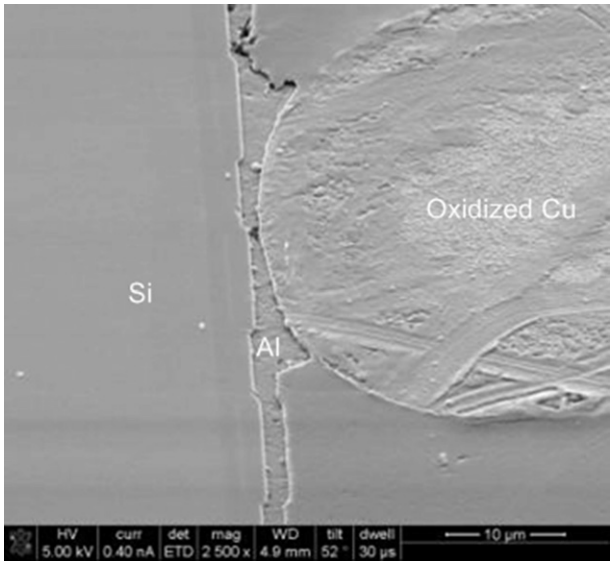

Fig. 2. Cross-sectional SEM image of Cu wire bonded sample fabricated with forming gas OFF.

polishing process. This, however, does not affect the Cu/Al interface. In Fig. 2, cross-section sample was rotated 90° in clockwise direction during SEM imaging. From Fig. 1, it is clearly seen that the Cu ball bond of sample with Forming Gas ON has a flat interface of Cu/Al. However, Fig. 2 shows the ball bond of sample with Forming Gas OFF is circular in shape and Al remnant under the ball bond has no significant thinning relative to portion which outside the ball bond area. This is due to that the cross-section of sample with Forming Gas OFF was not performed at a position close to the center of ball bond but at some distance near the edge of the ball bond. This could happen due to manual grinding and polishing during cross-section which has difficult to determine the position accurately. Moreover, positioning accuracy of cross-section is further affected by non-symmetrical ball bond. Common practice in performing cross-section is to grind and polish the sample until portion of wire above the bond is visible when it is close to center of ball bond. It is observed that non-symmetrical ball bond has much higher occurrence (~12%) in samples synthesized with Forming Gas OFF, as illustrated in Fig. 3. This non-symmetrical ball bond is not observed in sample synthesized with Forming Gas ON. This indicates that the sample with Forming Gas OFF has difficulty to achieve accurate cross-section positioning near to the center of ball bond. These nonsymmetrical ball bonds are originated from Cu FAB with "golf-clubbed" shape. The formation of this defective FAB is explained by Cu oxidation during EFO process that results in distortion of surface tension of molten Cu [13]. Fig. 4 illustrates the correlation between ball bond shape, cross-section positioning and expected result of cross-section. Mechanical pressure act on Cu FAB with "Golf-clubbed" shape through capillary results in non-symmetrical ball bond. Bonding interface of this type of ball bond is not centered around the axis along the length of Cu wire above the ball bond. This results in difficulty to judge the center position during mechanical cross-section. Cross-sectional view of the non-symmetrical ball bond shape leads to misinterpretation that Al remnant below ball bond is not thinned.

Synthesis of sample with Forming Gas OFF experiences high yield loss (yield <10%) attributed by Non Stick On Pad (NSOP) problem due to FAB oxidation as reported by Inderjit et al. [12]. This yield percentage is certainly not a manufacturing favorable situation and reveals the importance of Forming Gas supply. As mentioned above, oxide and contamination removal by ultrasonic energy is one of the critical parts that promote wire bonding [10]. In the case of Forming Gas OFF, a portion of ultrasonic energy will be used to remove additional Cu oxide layer on Cu FAB surface. This is believed to cause insufficient ultrasonic energy to promote bonding. With assumption of only little quantity of Cu FABs with thin oxide are available which ultrasonic energy provided is sufficient to cause breakdown of oxides at surfaces of FAB and Al bond pad metallization, it is expected low rate of successful bonding. This enables possible explanation of loss yield condition in the case of Forming Gas OFF.

Figs. 5 and 6 show the bright field TEM images of the lamella extracted from the samples synthesized with Forming Gas ON and OFF, respectively. It is observed in Fig. 5 that a relatively flat and uniform thickness of Al remnant is seen. On the other hand, Fig. 6 shows a significant thinning of Al remnant. This implies that the region of observation in Figs. 5 and 6 are belonging to center and periphery of the ball bond, respectively. Similar observation is found in Ref. [14]. Significant thinning of Al remnant at periphery of a ball bond is explained by higher stress distribution at this region [7]. This implies that direct comparison between Figs. 5 and 6 may not be possible, however, they provide fundamental information regarding IMC and voids condition for two combinations of location-Forming Gas supply.

From Fig. 6, the oxidized Cu ball bond with small voids distributed within it is clearly seen. This observation is not seen for non-oxidized Cu ball bond (with Forming Gas ON) as shown in Fig. 5. According to the study by Lee et al. [6], Cu FAB that experience intermediate oxidation will have small voids within it. However, for severely oxidized Cu FAB, the relatively bigger voids will be accumulated only near to the surface of Cu FAB and beneath the outer Cu oxide layer. It is believed that the formation of voids is due to air trap in insufficient protective environment. Therefore, it

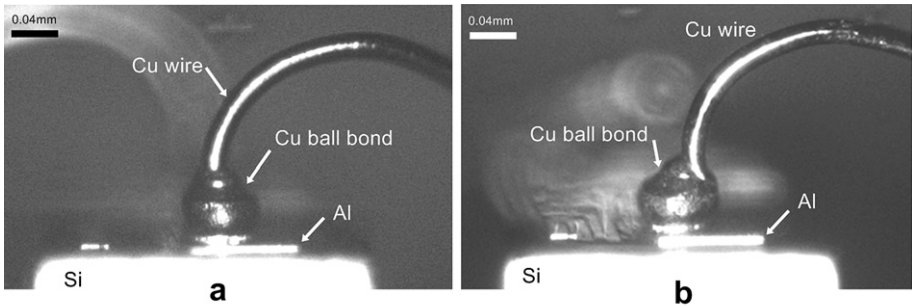

Fig. 3. Optical images of Cu ball bond of samples synthesized with (a) Forming gas ON, which is symmetrical in shape, (b) Forming gas OFF, which is non-symmetrical due to oxidation of FAB.

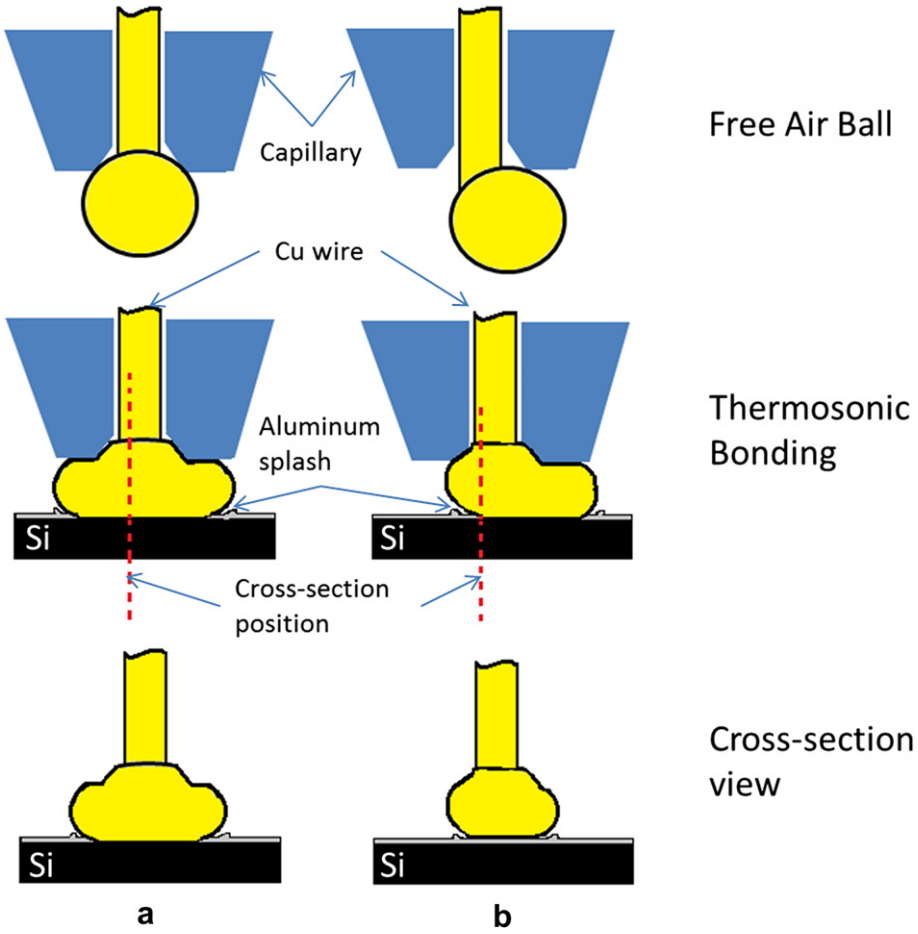

Fig. 4. Illustration of correlation between (a) Cu FAB shape (b) resultant ball bond shape with impression of Al remnant after cross-section.

is believed that the sample synthesized with Forming Gas OFF experience intermediate oxidation during its FAB formation.

From these TEM images, the Cu oxide layer is absent at the bonding interface. This means scrubbing of the Cu FAB against Al bond pad metallization during ultrasonic vibration had effectively removed oxides of Al and Cu. It is well known that ultrasonic vibration in Thermosonic bonding is capable to remove oxides and contamination at the bonding interface [2,10]. Native thin Al oxide layer on the surface bond pad metallization (~10 nm) is fragmented by ultrasonic scrubbing in Thermosonic bonding [2]. In Fig. 6, thick Al remnant on left is close to the edge of ball bond that is resulted from inaccurate position of cross-section. Besides, for both types of sample, there are some small voids present at the interface of Cu/Al as shown in Fig. 5(b), (d) and 6(a), (e). From Fig. 5(b), IMC does not form around the void. This is an indication that Cu and Al at this area are initially not in contact so that interdiffusion could not occur during ultrasonic welding. This void is unbonded area of the bonding interface. Wulff et al. [5] reports the similar unbonded area outside the nucleation points of IMC in Gold wire–Al bond pad system due to ununiformed ultrasonic energy transfer to the interface. It is also mentioned that such detection in Cu/Al system is uncertain with SEM. Hang et al. [7] reports that as-bonded Cu/Al samples are free from void or crack. This is due to limited resolution of the SEM used in their studies, which is further improved in our study using TEM.

On the other hand, it is observed in sample with Forming Gas OFF that the voids form between the IMC and Cu ball bond (Fig. 6(a) that corresponding to the area apart from the ball bond center and Fig. 6(e) which belong to bonding interface that close to center). This indicates that the metals are initially in contact which allows interdiffusion and thus bonding of metals. However, the formation of IMC in turn creates a volume difference between Cu-IMC that results in voiding [2].

From Figs. 5(a), (c) and 6(c), (d), IMC layer is formed at the bonding interface with non-uniform thickness and discontinuity along the interface is observed. Thickness of visible IMC of sample synthesized with Forming Gas OFF is relatively higher. Fig. 7 shows the comparison of visible IMC thickness of each category of samples. This is due to difference in cross-section position for both samples. Cross-section of sample with Forming Gas ON is more centered compare to another sample. Thus lamella prepared by FIB of the sample with Forming Gas ON carries information of the bonding interface at center of ball bond. On the other hand, lamella of sample with Forming Gas OFF is representing the bonding interface which is close to the edge of ball bond. According to Hang et al. [7], non-uniform stress distribution is observed under a ball bond due to non-uniform deformation of ball bond and dissimilarity of materials. It is generally accepted that higher stress is concentrated at the periphery of the bonding compare to center of the bonding [7], as illustrated in Fig. 8 which is modified from Ref. [7] for better understanding. Higher stress around the periphery facilitates the growth of IMC at this area relative to center of the bonding. This explains the reason of higher IMC thickness in Fig. 6(c) and (d). Similar IMC thickness difference at center and periphery of ball bond is observed in Ref. [14] which compares the microstructure at these two regions at Cu–Al bonding interface.

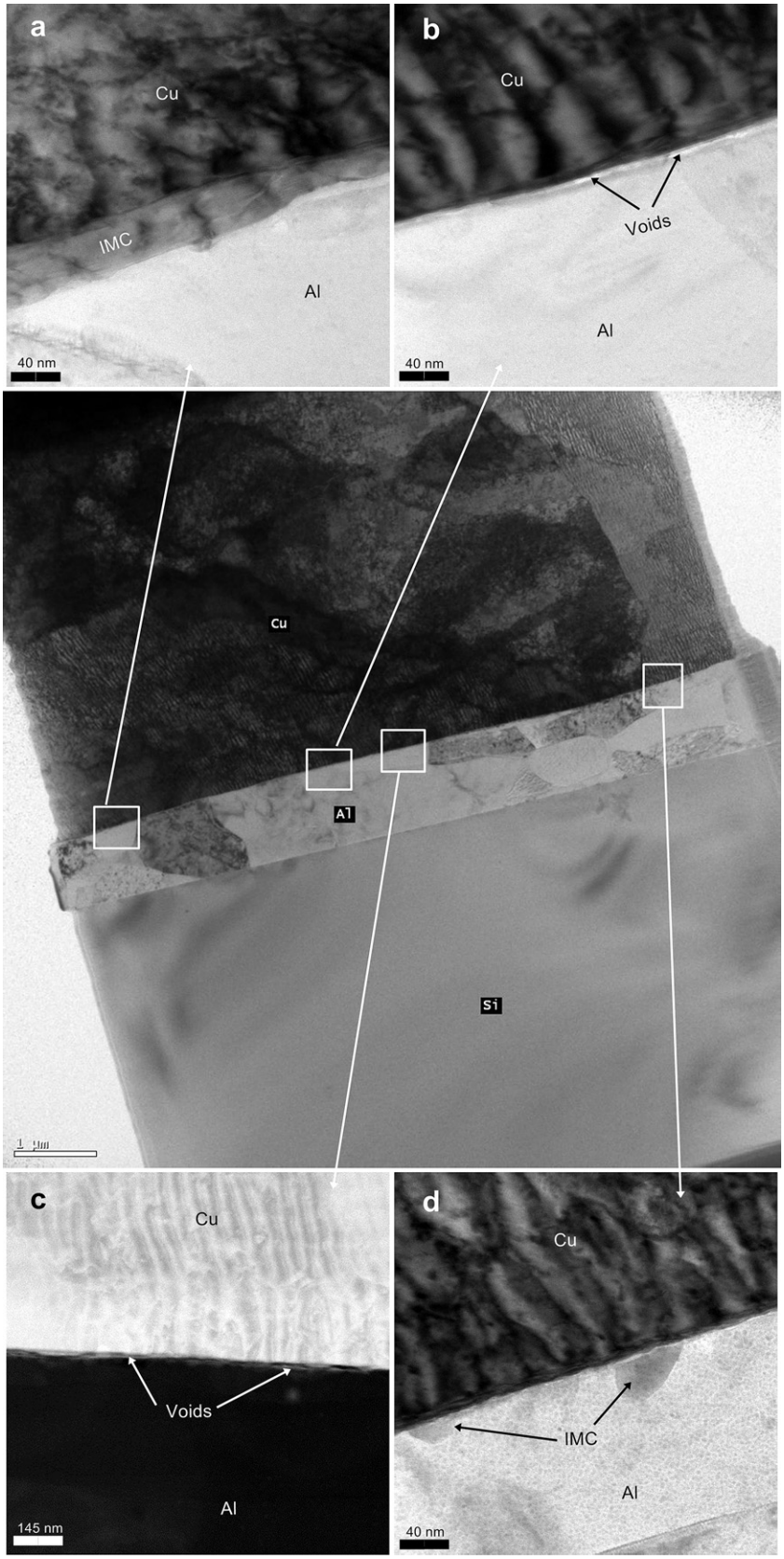

Fig. 5. Bright field TEM images of sample synthesized with forming gas ON. Insert (a) to (d) are magnified images which reveals the presence of IMC and voids. Insert (a), (b) and (d) are bright field images, while (c) is a dark field image.

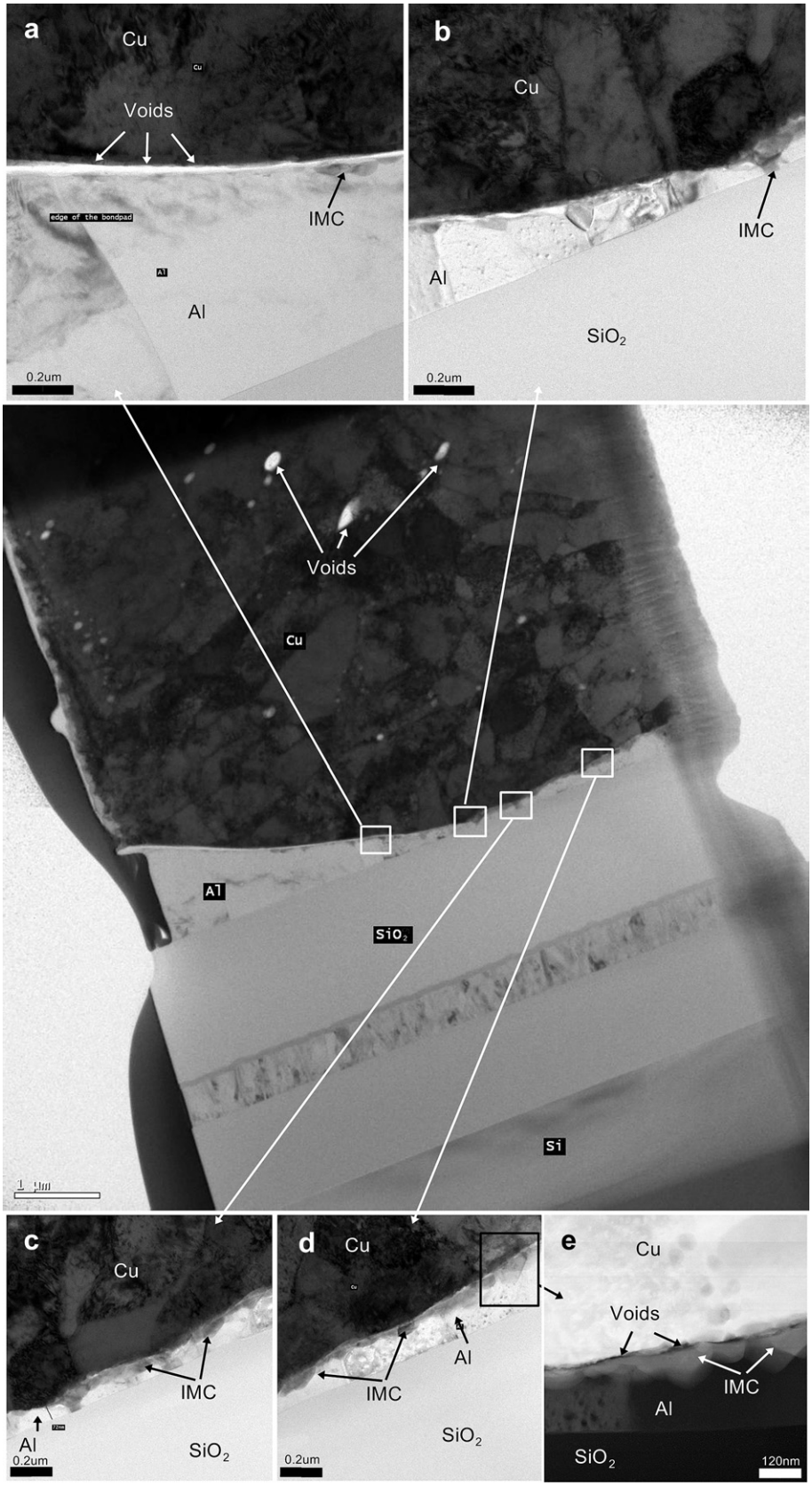

Fig. 6. Bright field TEM images of sample with forming gas OFF. Insert (a) to (d) are the magnified bright field images that reveals the presence of voids and IMC. Insert (e) shows a magnified dark field image from insert (d) that better visualize the presence of voids.

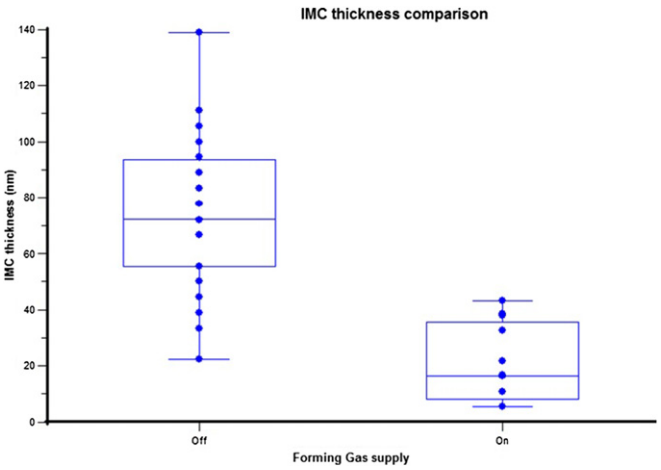

Fig. 7. Box plot to compare the IMC thickness of both samples synthesized with forming gas ON and OFF.

Fig. 9(a) and (b) compares the line scan EDX profile across the Cu/Al bonding interface of both samples that are synthesized with Forming Gas ON and OFF, respectively. From these EDX profile, it is noticed that signal intensity from Cu and Al is dominant across the interface. In Fig. 9(b), the intensity of Oxygen signal is higher at location of void. Existence of Oxygen in the void next to an obvious IMC suggests an initial contact of Oxides between Cu and Al. Besides, this oxide does not hinder the interdiffusion of Cu and Al atoms to form IMC. Similar detection of Oxygen element in the void at the interface of Cu/Al of as-bonded sample with Forming Gas supply is found in the work of Drozdov [15] that evident the minor oxide exists at the bonding interface. EDX signal intensity profile of Cu and Al that vary continuously across the interface shows a much slower signal intensity change (and thus composition change) at certain region indicating the existence of an approximate stoichiometric intermetallic phase. From Fig. 9(a), an IMC layer with total thickness ~14 nm consist of a phase with estimated composition (in at%) ratio of Al:Cu = 37:63 and thickness of ~3 nm. Similarly, in Fig. 9(b), a IMC layer with total thickness ~28 nm has a phase with estimated Al:Cu composition ratio and thickness of 60:40 and ~15 nm. The region outside the

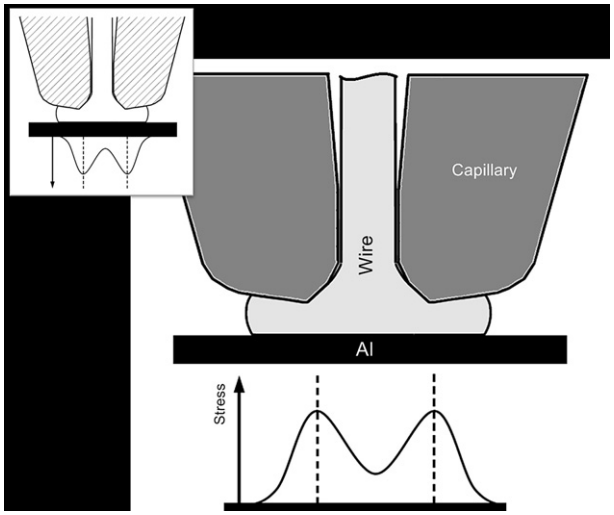

Fig. 8. Stress distribution under a ball bond during Thermosonic bonding. This figure is modified from Ref. [7] as shown in insert.

range of these phases belongs to solid solution of Al–Cu. The term of IMC used in previous sentences may not be accurate as the respective areas are interdiffusion zone at Cu/Al interface and the actual intermetallic phase is only a thin layer within the interdiffusion zone.

From Al–Cu binary phase diagram [16], these phases are Al_4Cu_9 (space group *P*-43*m*, Cubic) for sample with Forming Gas ON and AlCu (*C*12/*m*, Monoclinic) + $CuAl_2$ (3 possible space groups and structures: *P*4/*mmm* (tetragonal), *I*4/*mcm* (tetragonal)) and *Fmmm* (Orthorhombic) [2]) for sample with Forming Gas OFF. This finding is different from the Selective Area Diffraction phase identification in the study of Xu [2] and Drozdov [15] that shows Al_2Cu is the only phase formed in as-bonded Cu wire–Al bond pad metallization interface. This finding could be explained by higher frequency generated by ultrasonic transducer in the modern wire bonders in their studies. Modern wire bonders, i.e. K&S® 8082PPS in Ref. [14] and ASM® Eagle 60 in [2] and are equipped with transducer that are capable to generate 120 and 138 kHz [17] ultrasonic frequency, respectively. However, older model Shinkawa® ACB35 wire bonder used in this work is capable to generate only 60 kHz ultrasonic frequency. According to Ref. [10], effective heat of formation of phase Cu_9Al_4 and $CuAl_2$ are -41.6 J g^{-1} and -18.39 J g^{-1}, respectively. Phase with lower heat of formation tends to form first. It is expected that mentioned modern wire bonders are capable to generate higher ultrasonic energy to promote formation of $CuAl_2$ phase while older equipment could only promote formation of Cu_9Al_4 phase which requires lower energy.

Ball shear test is a promising technique to examine the mechanical strength of the bonding interface [8] and it is widely used by industry. Fig. 10 shows the result of ball shear strength per unit area comparison of both sample synthesized with Forming Gas ON and OFF. Sample size involved is 30 pieces of unit for each sample type. Average ball shear strengths for both samples synthesized with Forming Gas ON and OFF are 21,461 g mm^{-2} and 17,375 g mm^{-2}, respectively. Ball shear failure mode observed for both samples is categorized as bond lift. In general, bond lift failure mode in ball shear test is a phenomenon that ball bond is separated from bond pad metallization upon shearing. In this mode, Cu–Al bonding interface is the weakest portion in the system during shearing [18]. Higher ball shear strength (force per unit area) indicates that IMC thickness is higher [19] in sample synthesized with Forming Gas ON, though this thicker IMC layer is not seen in TEM images (Fig. 5). This is because the position of images is localized at center region of the ball bond which develops thinner IMC compare to the periphery. From TEM images from Ref. [14], thick IMC is found at periphery while thin and discontinued IMC located at the center of the ball bond. From their result, thickness of IMC at periphery can be 2 times greater than that at the center region of the ball bond. This is due to non-uniform stress distribution under the ball bond [7] as explained in previous section. It is commonly observed that the IMC/phase growth of Cu/Al in an electronic microchip after annealing process is complying parabolic law due to volume diffusion of elements into each other [20,21]. In this case, interfacial bonding temperature could be deduced from the thickness of an intermetallic phase could be described by the following empirical equation of volume diffusion [22] (all variables in S.I. units).

For single phase system, i.e. sample with Forming Gas ON consisting Cu9Al4 phase,

$$W = k\sqrt{t} \tag{1}$$

where k = growth rate constant ($ms^{-1/2}$); t = time of diffusion in seconds (in this case, duration of thermosonic bonding).

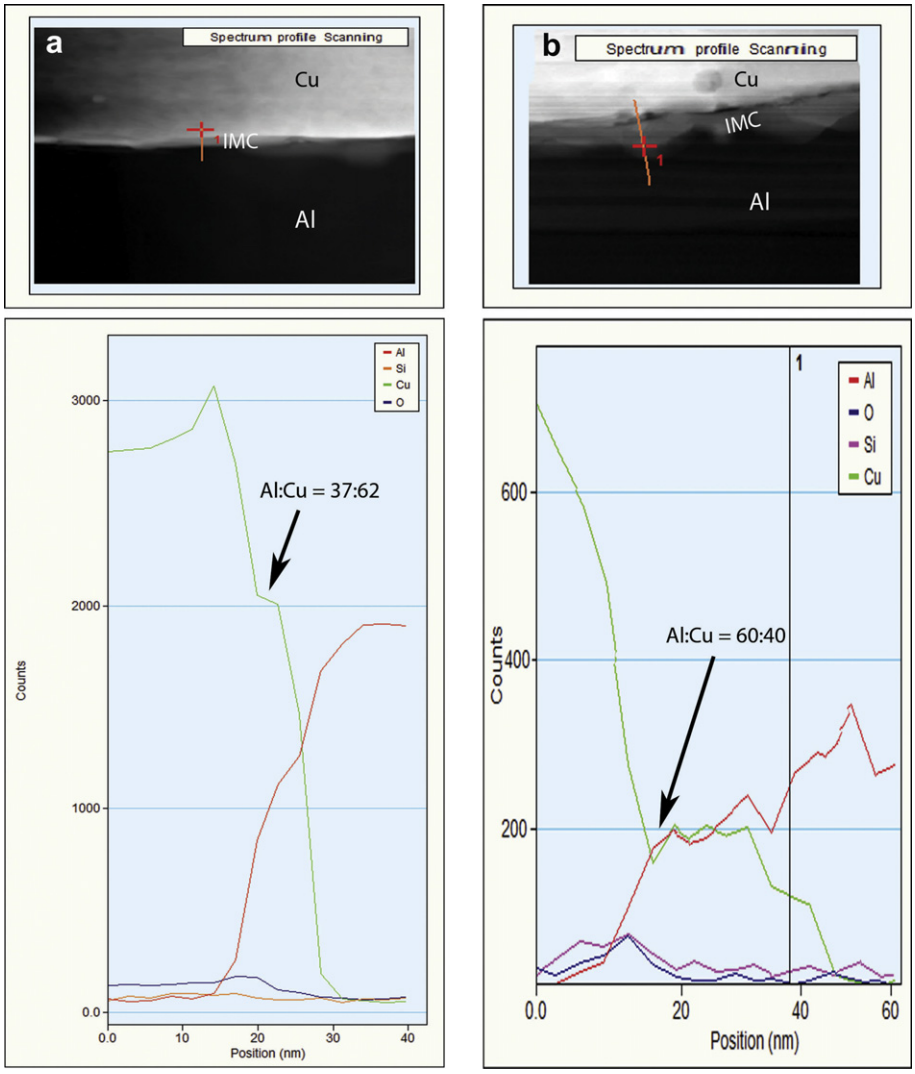

Fig. 9. Line scan EDX across Cu–Al interface for sample synthesized with (a) Forming gas ON and (b) Forming gas OFF.

For Cu_9Al_4 phase,

$$k^2 = 3.2 \times 10^{-6} \times \exp\left(-\frac{132214.4}{RT}\right)\ \mathrm{m^2 s^{-1}} \quad (2)$$

where R = gas constant = 8.3145 $\mathrm{JK^{-1}mol^{-1}}$, T = absolute temperature (K).

Rearrange the equations, one will have

$$T = \frac{132214.4}{R\ln\left(\frac{3.2 \times 10^{-6} t}{W^2}\right)}\ \mathrm{K} \quad (3)$$

With these equations, intermetallic phase thickness measurement and ultrasonic scrubbing time of 15 milliseconds (ms), the estimated temperature at the interface of Cu/Al is about 710 K or 437 °C. The ultrasonic energy promotes additional 157 °C at the bonding interface.

For mixed phases of CuAl and $CuAl_2$, one may assume the total thickness of intermetallic phases that consists of 2 phases as an arithmetic summation of thickness of individual phase,

$$W = W_{\mathrm{CuAl}} + W_{\mathrm{CuAl_2}} \quad (4)$$

$$W = (k_{\mathrm{CuAl}} + k_{\mathrm{CuAl_2}})\sqrt{t} \quad (5)$$

From Ref. [20] again,

$$k_{\mathrm{CuAl}} = 1.7 \times 10^{-10} \times \exp\left(-\frac{82006.4}{RT}\right)\ \mathrm{m^2 s^{-1}} \quad (6)$$

$$k_{\mathrm{CuAl_2}} = 9.1 \times 10^{-7} \times \exp\left(-\frac{122591.2}{RT}\right)\ \mathrm{m^2 s^{-1}} \quad (7)$$

From Eqs. (5)–(7), by substituting thickness of phases and ultrasonic scrubbing time, the equation will eventually become the following form:

$$0 = A + B\exp(xT) + C\exp(yT) \quad (8)$$

where $A = -(W/\sqrt{t}) = -1.2247 \times 10^{-7}\ \mathrm{ms^{-1/2}}$, B = Square root of coefficient in Eq. (6) = $1.3038 \times 10^{-5}\ \mathrm{ms^{-1/2}}$; C = Square root of coefficient in Eq. (7) = $9.5394 \times 10^{-4}\ \mathrm{ms^{-1/2}}$; x = reciprocal of exponential coefficient in Eq. (6) = $2R/82006.4 = 2.0278 \times 10^{-4}\ \mathrm{K^{-1}}$; y = reciprocal of exponential coefficient in Eq. (7) = $2R/122591.2 = 1.3565 \times 10^{-4}\ \mathrm{K^{-1}}$.

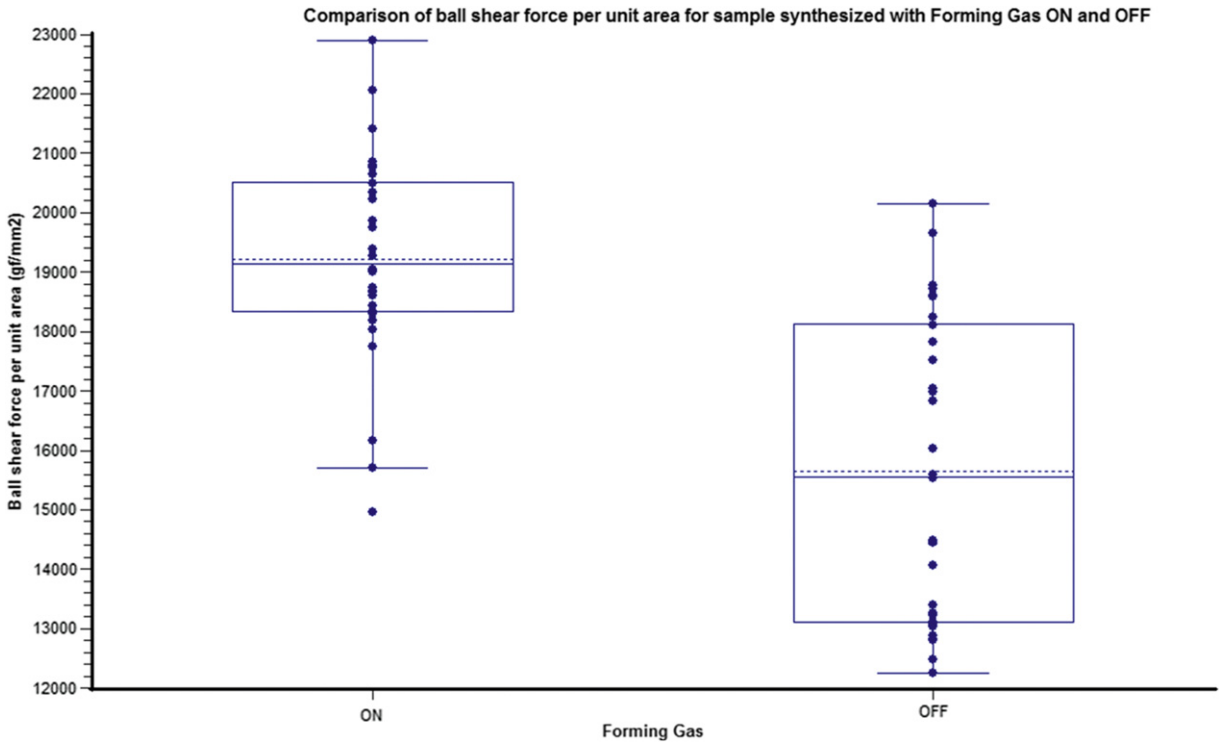

Fig. 10. Box plot of ball shear strength for both type of sample.

Eq. (8) can be solved graphically or numerically. However, one may not find a valid real solution for above equation. This indicates that the multi-phase interdiffusion system may be more complicated than arithmetic summation of individual phase. Alternatively, the failure of model based on volume diffusion of individual phase may be attributed from different diffusion mechanism of the elements, e.g. Grain Boundary diffusion, though this is not observed in the limited sample size in this study. In the report of morphological and chemical studies by Drozdov et al. [14], it is highlighted that an isolated $CuAl_2$ grain exists within Al bond pad metallization at the center of as-bonded sample. The possible explanation given in their report is that Cu atoms diffuse into Al by Grain Boundary diffusion mechanism.

4. Conclusion

In this study, samples with Cu wire bonded on pure Al bond pad metallization are synthesized with both condition of Forming Gas ON and OFF to control the oxidation of Cu FAB. SEM study reveals that offset in cross-section position in the sample synthesized with Forming Gas OFF. This is due to accuracy of mechanical cross-section and non-symmetrical oxidized ball bond. TEM study at the bonding interface shows the IMC present in as-bonded sample and Cu ball bond with Forming Gas OFF is intermediately oxidized. Line-scan EDX reveals that the IMC actually consist of interdiffusion zone and a distinctive thin layer of intermetallic phase. The intermetallic phase in the Forming Gas ON sample consists of 3 nm Al_4Cu_9, and 15 nm of CuAl and $CuAl_2$ mixture in another sample. Existence of Cu oxide layer on the Cu FAB surface (due to Forming Gas OFF) does not hinder the bonding as it is removed by scrubbing of ultrasonic vibration. Small voids are observed at the bonding interface for the Forming Gas ON samples belongs to unbonded area. Voiding at the bonding interface of the Forming Gas OFF sample is due to volumetric shrinkage of phase formation. Intermetallic phase thickness, bond time and volume diffusion empirical equations are used to estimate the temperature raise at the bonding interface. It is estimated the interface temperature of as-bonded sample with Forming Gas ON is about 437 °C. Similar approach to estimate the interface temperature for sample synthesized with Forming Gas OFF which consists of mixed intermetallic phases leads to imaginary solution of temperature. This indicates that phase development in multi-phase system is more complicated than arithmetic summation of individual phase. Alternatively, different diffusion mechanism could be the main factor that results in failure of the mathematical model.

Acknowledgement

Authors thank Ms. Lee C.Y. and Mr. Lee C.C. from Infineon (Malaysia) Sdn. Bhd. for assisting in sample preparation. Assistance from Mr. Tang L.J. from Institute of Microelectronic, Singapore for analytical analysis is appreciated. This study has been supported by Infineon (Melaka, Malaysia) Sdn. Bhd and Universiti Teknikal Malaysia Melaka (UTeM), Malaysia.

Appendix A. Supplementary material

Supplementary data related to this article can be found online at http://dx.doi.org/10.1016/j.matchemphys.2012.07.036.

References

[1] J. Onuki, M. Koizumi, I. Araki, IEEE Trans. Compon. Hybrids Manuf. Technol. 10 (1987) 550–555.
[2] H. Xu, C. Liu, V.V. Silberschmidt, S.S. Pramana, T.J. White, Z. Chen, V.L. Acoff, Acta Mater. 59 (2011) 5661–5673.
[3] W.D. Calister Jr., Materials Science and Engineering an Introduction, sixth ed. John Wiley & Sons Inc., New York, 2004.
[4] D. Micheal, L. Levine, 29th Int. Electron. Manuf. Technol. Symp., California, 14–16th July 2004, 186–190.
[5] F.W. Wulff, C.D. Breach, D. Stephen, K.J. Dittmer Saraswati, 6th Proc. of Electron. Packag. Technol. Conf., 8–10 Dec. 2004, 348–353.

[6] C.Y. Lee, C.C. Lee, C.C. Lim, 2nd Tech. Symp. Infineon Technology Sdn. Bhd., Malacca, Malaysia, 24–28 August 2009.
[7] C.J. Hang, C.Q. Wang, M. Mayer, Y.H. Tian, Y. Zhou, H.H. Wang, Microelectron. Reliab. 48 (2008) 416–424.
[8] G.E. Servais, S.D. Brandenburg, 17th Int. Symp. for Test. and Fail. Anal., Los Angeles, 11–15 November 1991, 525–529.
[9] H. Clauberg, P. Backus, B. Chylak, Microelectron. Reliab. 51 (2011) 75–80.
[10] C.D. Breach, F.W. Wulff, Microelectron. Reliab. 50 (2010) 1–20.
[11] L.T. Nguyen, D. McDonald, A.R. Danker, P. Ng, IEEE Trans. Comp. Pack. Manuf. Technol. 18 (1995) 423–429.
[12] S. Inderjit, J.Y. On, L. Levine, 55th Proc. of Electron. Comp. and Technol. Conf., 31st May–3rd June 2005, 843–847.
[13] A. Pequegnat, H.J. Kim, M. Mayer, Y. Zhou, J. Persic, J.T. Moon, Microelectron. Reliab. 51 (2011) 43–52.
[14] Y.Y. Tan, F.K. Yong, 17th IEEE Int. Symp. on the Phys. and Fail. Anal. of Integr. Circuit, Singapore, 5–9 July 2010, 1–4.
[15] M. Drozdov, G. Gur, Z. Atzmon, W.D. Kaplan, J. Mater. Sci. 43 (2008) 6029–6037.
[16] J.L. Murray, Int. Mat. Rev. 30 (1985) 211–234.
[17] F. Wulff, C.W. Tok, C.D. Breach, Mater. Lett. 61 (2007) 452.
[18] L. England, T. Jiang, 57th Electron. Comp. and Technol. Conf., Nevada, USA, 29 May–1st June 2007.
[19] H. Xu, C. Liu, V.V. Silberschmidt, Z. Chen, Scripta Mater. 61 (2009) 165–168.
[20] H.J. Kim, J.Y. Lee, K.W. Paik, K.W. Koh, J. Won, S. Choe, J. Lee, J.T. Moon, Y.J. Park, IEEE Trans. Comp. Pack. Technol. 26 (2003) 367–374.
[21] H. Xu, C. Liu, V.V. Silberschmidt, Z. Chen, J. Electron. Mater. 39 (2010) 124–131.
[22] Y. Funamizu, K. Watanabe, Trans. Jpn. Inst. Metal. 12 (1971) 147–152.